Atmospheric CO2 and Climate on Millennial Time Scales During the Last Glacial Period

Jinho Ahn, *et al.*

Science **322**, 83 (2008);
DOI: 10.1126/science.1160832

dered compared with bulk water, consistent with the dynamics of water molecules in proximity to small hydrophobic groups (*31*). The confined and interfacial water are prevalent in biological systems, such as the water in ion channels and in proximity to proteins. The affinity change due to temperature-induced structural change of water could be relevant to various phenomena, including in biological systems, such as the cold denaturation of proteins (*2*).

References and Notes

1. D. Chandler, *Nature* **437**, 640 (2005).
2. C. J. Tsai, J. V. Maizel, R. Nussinov, *Crit. Rev. Biochem. Mol. Biol.* **37**, 55 (2002).
3. G. Hummer, J. C. Rasaiah, J. P. Noworyta, *Nature* **414**, 188 (2001).
4. K. Koga, G. T. Gao, H. Tanaka, X. C. Zeng, *Physica A* **314**, 462 (2002).
5. R. J. Mashl, S. Joseph, N. R. Aluru, E. Jakobsson, *Nano Lett.* **3**, 589 (2003).
6. A. I. Kolesnikov *et al.*, *Phys. Rev. Lett.* **93**, 035503 (2004).
7. Y. Maniwa *et al.*, *Chem. Phys. Lett.* **401**, 534 (2005).
8. A. Striolo *et al.*, *Adsorption* **11**, 397 (2005).
9. J. K. Holt *et al.*, *Science* **312**, 1034 (2006).
10. S. H. Mao, A. Kleinhammes, Y. Wu, *Chem. Phys. Lett.* **421**, 513 (2006).
11. Q. Chen *et al.*, *Nano Lett.* **8**, 1902 (2008).
12. R. S. Vartapetyan, A. M. Voloshchuk, *Usp. Khim.* **64**, 1055 (1995).
13. T. Ohba, H. Kanoh, K. Kaneko, *J. Am. Chem. Soc.* **126**, 1560 (2004).
14. X. P. Tang *et al.*, *Science* **288**, 492 (2000).
15. Materials and methods are available as supporting material on *Science* Online.
16. A. Kleinhammes *et al.*, *Phys. Rev. B* **68**, 075418 (2003).
17. H. Z. Geng *et al.*, *Chem. Phys. Lett.* **399**, 109 (2004).
18. Y. Maniwa *et al.*, *Nat. Mater.* **6**, 135 (2007).
19. S. J. Gregg, K. S. W. Sing, *Adsorption, Surface Area, and Porosity* (Academic Press, London, New York, ed. 2, 1982).
20. J. Pires, M. L. Pinto, A. Carvalho, M. B. de Carvalho, *Adsorption* **9**, 303 (2003).
21. T. R. Jensen *et al.*, *Phys. Rev. Lett.* **90**, 086101 (2003).
22. O. Byl *et al.*, *J. Am. Chem. Soc.* **128**, 12090 (2006).
23. D. Beaglehole, H. K. Christenson, *J. Phys. Chem.* **96**, 3395 (1992).
24. G. R. Birkett, D. D. Do, *J. Phys. Chem. C* **111**, 5735 (2007).
25. T. Kurita, S. Okada, A. Oshiyama, *Phys. Rev. B* **75**, 205424 (2007).
26. D. Takaiwa, I. Hatano, K. Koga, H. Tanaka, *Proc. Natl. Acad. Sci. U.S.A.* **105**, 39 (2008).
27. A. Abragam, *The Principles of Nuclear Magnetism* (Clarendon Press, Oxford, 1961).
28. R. Kubo, K. Tomita, *J. Phys. Soc. Jpn.* **9**, 888 (1954).
29. J. P. Korb, S. Xu, J. Jonas, *J. Chem. Phys.* **98**, 2411 (1993).
30. J. Baugh *et al.*, *Science* **294**, 1505 (2001).
31. Y. L. A. Rezus, H. J. Bakker, *Phys. Rev. Lett.* **99**, 148301 (2007).

32. This work was supported by NSF under contract DMR 0513915. We thank O. Zhou for help in SWNTs synthesis.

Supporting Online Material

www.sciencemag.org/cgi/content/full/322/5898/80/DC1
Figs. S1 and S2

26 June 2008; accepted 19 August 2008
10.1126/science.1162412

Atmospheric CO_2 and Climate on Millennial Time Scales During the Last Glacial Period

Jinho Ahn* and Edward J. Brook

Reconstructions of ancient atmospheric carbon dioxide (CO_2) variations help us better understand how the global carbon cycle and climate are linked. We compared CO_2 variations on millennial time scales between 20,000 and 90,000 years ago with an Antarctic temperature proxy and records of abrupt climate change in the Northern Hemisphere. CO_2 concentration and Antarctic temperature were positively correlated over millennial-scale climate cycles, implying a strong connection to Southern Ocean processes. Evidence from marine sediment proxies indicates that CO_2 concentration rose most rapidly when North Atlantic Deep Water shoaled and stratification in the Southern Ocean was reduced. These increases in CO_2 concentration occurred during stadial (cold) periods in the Northern Hemisphere, several thousand years before abrupt warming events in Greenland.

The last glacial period was characterized by abrupt climate and environmental changes on millennial time scales. Prominent examples include abrupt warming and cooling in Greenland ice core records (Dansgaard-Oeschger, or DO, events) (*1*, *2*) and abrupt iceberg discharges in the North Atlantic (Heinrich, or H, events) (*3*), the latter appearing to predate the longest and largest DO events (Fig. 1A). Age synchronization between Greenland and Antarctic ice cores through atmospheric CH_4 variations reveals that Antarctic and Greenlandic temperature are linked, but not in phase (*4*, *5*) (Fig. 1, A, B, and D). Antarctic warming started before warming in Greenland for most of the large millennial events in the records, and Antarctic temperatures began to decline when Greenland rapidly warmed. Model and ice core studies suggest that this link is maintained by changes in meridional overturning circulation (*6*, *7*).

In contrast to the interhemispheric climate link, the relation between atmospheric CO_2 and climate, in the glacial period [~20 to 120 thousand years ago (ka)], has not been as well documented because of scatter in data sets (*8*) and/or chronological uncertainties (*9*). Understanding CO_2 variability is important, however, because of the direct role of CO_2 as a greenhouse gas and the probable influence of changes in ocean circulation on past atmospheric CO_2 concentrations. Here, we provide high-resolution atmospheric CO_2 data from the Byrd ice core (*10*), with a chronology well synchronized with the Greenland ice cores via CH_4 correlation (*4*). The data cover the period of 20 to 90 ka (Fig. 1C), including previously published results for 47 to 65 ka (*11*). We also measured CH_4 in 36 samples from Byrd to better constrain the chronology of the 67- to 87-ka time period [the time of DO-19, 20, and 21 and Antarctic events A5 to A7 (*4*)] (Fig. 1D). Rapid increases in CH_4 concentration are essentially synchronous with abrupt warming in Greenland within decades (*12*–*14*). With CH_4 and CO_2 data from the same core, and in many cases from the same samples, we could directly study the phasing between CO_2 and Greenland temperature variations, circumventing uncertainties due to age differences between ice and gas in ice core records (*12*–*14*).

We call attention to two distinct features of atmospheric CO_2 variations associated with climate changes in the Northern and Southern Hemispheres. First, CO_2 variation is strongly correlated with $\delta^{18}O_{ice}$ in the Byrd core, a proxy for site temperature, but whereas CO_2 remained relatively stable for about 1 to 2 ka after reaching maximum levels associated with peaks in Antarctic warming, Antarctic temperature dropped rapidly (Fig. 1, B and C, and fig. S1). In contrast to the slow decline of CO_2 relative to Antarctic cooling, the onsets of CO_2 increases are generally synchronous with Antarctic warming within data and age uncertainties (fig. S1).

Second, an increase in CO_2 predates, by 2 to 5 ka, the abrupt warming in Greenland associated with DO events, 8, 12, 14, 17, 20 and 21, the largest and longest abrupt events in the Greenland record over this time period (Figs. 1, A and C, and 2) (DO-19 may be an exception, but the timing of the onset of CO_2 rise is difficult to determine). The CO_2 increase slowed just after the abrupt warming of those events. We do not resolve any similar CO_2 variability associated with the shorter DO climate oscillations in the 37- to 65-ka period (DO-9, 11, 13, 15) with the current data set, but small variations associated with the shorter DO cycles cannot be excluded. Between 19 and 37 ka, there are some variations that may be associated with DO events 2 to 7, particularly a CO_2 peak at ~ 28 ka, which may be related to DO-4 and the stadial period preceding it. Higher-resolution data will be needed to further understand this variability.

Models of millennial-scale CO_2 variations suggest that changes in North Atlantic Deep

Department of Geosciences, Oregon State University, Corvallis, OR 97331–5506, USA.

*To whom correspondence should be addressed. E-mail: jinhoahn@gmail.com

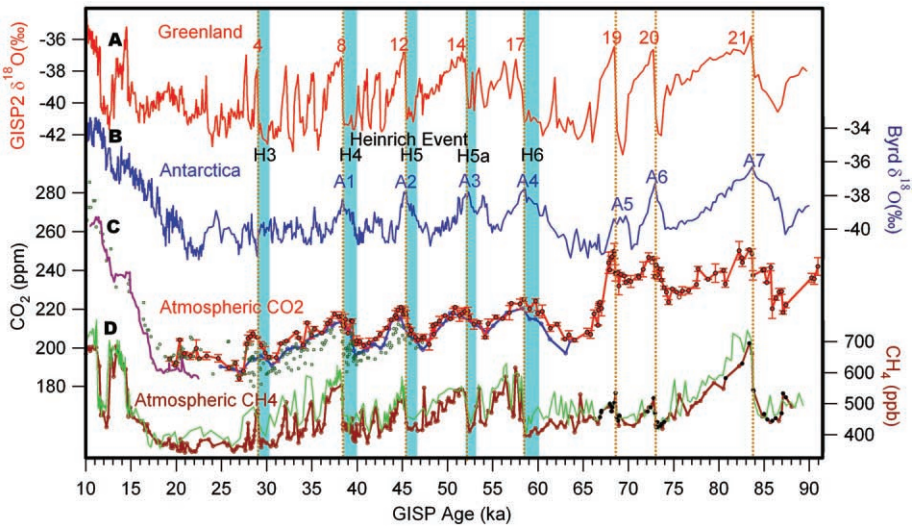

Fig. 1. Atmospheric CO_2 composition and climate during the last glacial period. (**A**) Greenlandic temperature proxy, $\delta^{18}O_{ice}$ (*2*). Red numbers denote DO events. (**B**) Byrd Station, Antarctica temperature proxy, $\delta^{18}O_{ice}$ (*4*). A1 to A7, Antarctic warming events (*4*). (**C**) Atmospheric CO_2 concentrations. Red dots [this study and early results for 47 to 65 ka (*11*) at Oregon State University] and green circles (*8*) (results from University of Bern) are from Byrd ice cores. Red dots are averages of replicates, and red open circles at ~73 and 76 ka are single data [this study and (*11*)]. The chronology used for Byrd CO_2 is described in (*10*). Blue line is from Taylor Dome ice core (*9*) on the GISP2 time scale (*11*). Purple line is from EPICA Dome C (*27*). (**D**) CH_4 concentrations from Greenland (green) (*4*) and Byrd ice cores (brown) [(*4*) and this study]. Black dots, new measurements for this study. Vertical blue bars, timing of Heinrich events (H3 to H6) (*25*, *26*). Brown dotted lines, abrupt warming in Greenland.

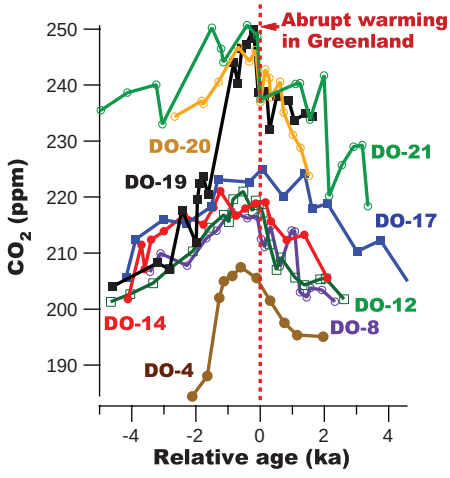

Fig. 2. Atmospheric CO_2 variations relative to abrupt warming in Greenland. The sequence of Byrd CO_2 variations [this study and (*11*)] associated with each DO event is numbered. Red dotted line indicates the timing of the abrupt warming in Greenland defined by the rapid rise in CH_4 concentration in the Byrd ice core.

Water (NADW) formation can affect atmospheric CO_2 concentration through both physical and biological processes in the ocean and terrestrial biosphere. Comparing model results is difficult because of differences in boundary conditions, amount and duration of freshwater forcing, and treatment of the terrestrial biosphere and other relevant processes. Model results suggest that several different mechanisms may relate changes in NADW to changes in atmospheric CO_2 concentration, including increases in Southern Ocean sea surface temperatures and decreased salinity in the North Atlantic (*15*), and reduced Southern Ocean stratification and release of CO_2 (*16*). Climate-induced changes in the terrestrial biosphere caused by changes in ocean circulation may also affect the atmospheric CO_2 (*17*, *18*), but the magnitude of this effect is not yet clear.

To explore the possible link between ocean circulation and CO_2, we compared our data with the benthic foraminiferal $\delta^{13}C$ from Iberian margin sediments at depth of 3146 m, using $\delta^{13}C$ as a proxy for the balance between northern source and southern source deep waters at this site (*19*) (Fig. 3C). We also used bulk sediment $\delta^{15}N$ from the Chile margin in intermediate depths as a proxy for input of the Subantarctic Mode Water to this region (*20*). Following (*20*), we interpreted this proxy as an indicator of the reduction of stratification in the Southern Ocean (Fig. 3D), which may result from changes in NADW. The two data sets are inversely correlated (note the reverse scale of the $\delta^{13}C$) in most time intervals, implying that shoaling NADW is linked to reduction of stratification in the Southern Ocean. The rate of change of CO_2 concentration peaks when these proxies indicate a maximum in NADW shoaling and reduction of stratification in the Southern Ocean (Fig. 3, B to D), implying CO_2 release to the atmosphere during maxima in Southern Ocean destratification, as suggested in model experiments (*16*). At around 19 to 37 ka, the correlations among the two marine proxies and the rate of change of CO_2 are not as clear as they are in the 37- to 91-ka time period. Other, perhaps longer-term processes may have controlled atmospheric CO_2 during this time period. Alternatively, the geochemical proxies plotted in Fig. 3 may not directly reflect millennial change in ocean circulation as climate approached the last glacial maximum. Models of long-term glacial-interglacial CO_2 variations indicate that destratification in the Southern Ocean should cause CO_2 to increase (*21*, *22*), although it is not clear if these model results are directly applicable to millennial-scale variations. Other mechanisms that may contribute to glacial-interglacial cycles and may be important on millennial time scales include changes in CO_2 outgassing due to variations in sea ice extent (*23*) and changes in iron fertilization (*24*) in the Southern Ocean.

Heinrich events are associated with the cold periods before major DO events, and one scenario that could explain CO_2 variations is that large freshwater fluxes associated with Heinrich events cause changes in ocean circulation and release of CO_2 to the atmosphere through mechanisms discussed above (*15*, *16*). However, based on existing age constraints (*3*, *25*, *26*), H events 3, 4, 5, 5a, and 6 appear to have occurred 0 to 3 ka after CO_2 started to rise (Fig. 1 and fig. S2). Unfortunately, precise comparison of CO_2 and all of the H events is prevented by chronological uncertainties. In some cases the relative timing of H events and events in the ice core record can be constrained via correlations between temperature proxies in marine records and ice core data, and identification of ash layers (*3*, *25*, *26*). For example, the abrupt warming at DO-15 (defined by the rapid rise in CH_4 concentration, fig. S2) has a correlative feature in North Atlantic sediment records (*26*) and occurred before H5a, whereas the CO_2 rise associated with A3 started during or before DO-15, and therefore also before H-5a. However, for other H events, the timing of the associated CO_2 rise cannot be precisely determined in this way given the current time resolution of the ice core records.

The data also indicate abrupt increases in CO_2 concentration of ~10 parts per million (ppm) at the times of abrupt warming associated with DO-19, 20, and 21 (Figs. 1 and 2). The magnitude of these jumps is similar to those during the last Termination (*27*), when the CO_2 level and temperature are similar to those of DO-19, 20, and 21 (65 to 90 ka). During the intervening period (20 to 65 ka), this type of variability is not as apparent in our record. The origin of these brief periods of elevated CO_2 is not clear, but may be related to increases in sea surface temperature in the Northern Hemisphere or release of CO_2 from the terrestrial biosphere by respiration, associated with abrupt warming in Greenland.

Another notable feature is the rapid decrease in CO_2 concentration of ~43 ppm at ~68 ka [Greenland Ice Sheet Project 2 (GISP2) time scale] after DO-19 (Figs. 1C and 4). The magnitude of the CO_2 drop is about half the total CO_2

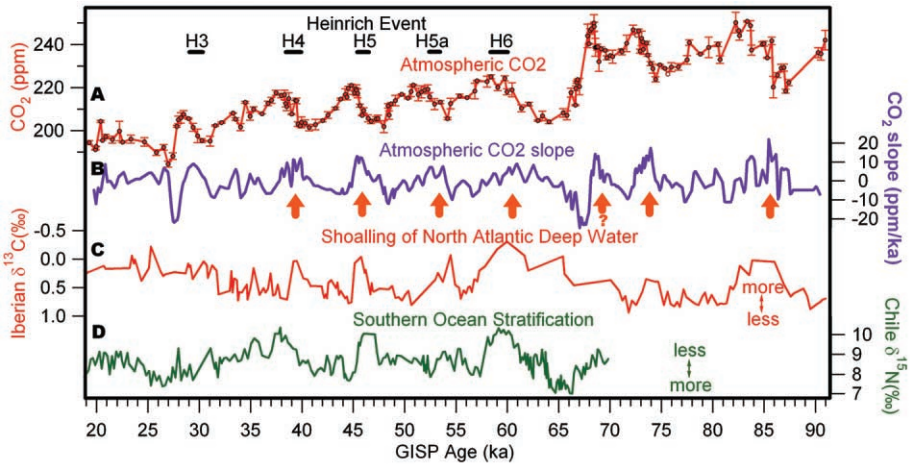

Fig. 3. Atmospheric CO_2 and change in ocean circulation. (**A**) Atmospheric CO_2 concentrations from the Antarctic Byrd ice core [this study and (*11*)], measured at Oregon State University (table S1). (**B**) Derivative of the Byrd CO_2 concentrations shown in (A). Nine-point running mean of the first derivative is calculated from data interpolated to 100-year spacing. (**C**) Benthic foraminifera (*Cibicidoides* wuellerstorfi) $\delta^{13}C$ from the Iberian margin sediment core (*19*). Ages are synchronized by correlation between planktonic foraminifera from the same sediment core and Greenland $\delta^{18}O_{ice}$ (*19*). (**D**) Bulk sediment $\delta^{15}N$ from the Chile Margin as a proxy for the reduction of the Southern Ocean stratification (*20*). Ages are synchronized by benthic foraminifera $\delta^{18}O$ correlation with that from Iberian margin (*20*). Orange arrows show the positive correlation between CO_2 derivative and reduced stratification in the Southern Ocean or shoaling NADW. The arrow with a question mark indicates an unclear correlation due to lack of resolution in the $\delta^{13}C$ record. Horizontal black bars, timing of Heinrich events (H3 to H6) (*25*, *26*).

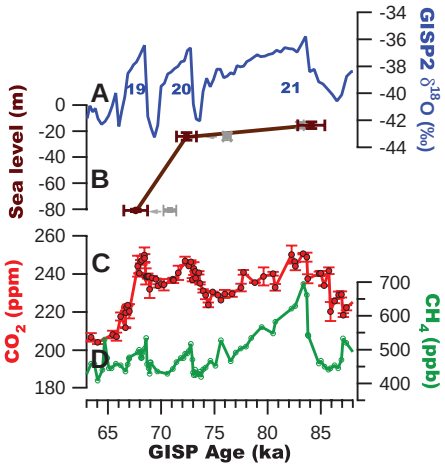

Fig. 4. Comparison of the rapid drop in CO_2 concentration with coral sea-level proxy. (**A**) Greenland temperature proxy (*2*). Blue numbers denote DO events. (**B**) Coral sea-level records (*33*). Original U-Th absolute ages (*33*) (gray dots) are adjusted to the GISP2 time scale (brown dots) by means of the correlations between Sanbao speleothem $\delta^{18}O$ (*34*) and GISP2 $\delta^{18}O_{ice}$ (*2*). The sea-level age uncertainties on the GISP2 time scale were calculated with age uncertainties from coral U-Th (±0.3 to 0.6 ka) and speleothem U-Th (±0.5 to 0.65 ka), and correlations between GISP2 and speleothem $\delta^{18}O$ (±0.5 to 1.0 ka) and between GISP2 $\delta^{18}O_{ice}$ and Byrd CO_2 records (±0.3 to 0.5 ka). (**C**) Atmospheric CO_2 concentration from Byrd ice core [this study and (*11*)]. (**D**) Atmospheric CH_4 concentration from Byrd ice core [(*4*) and this study].

variations during long-term glacial-interglacial cycles. The fastest rate of decrease during the event is ~11 ppm/ka, but the true value could have been even larger. A similar decrease of ~40 ppm at this time is also observed in low-resolution Vostok (*28*) and Dome Fuji records (*29*). A large sea-level drop appears to predate the CO_2 decline (Fig. 4). It is notable that a rapid increase of dust flux occurred in the equatorial Pacific and Antarctica at around the same time (*30*, *31*).

Our results support the idea that atmospheric CO_2 concentration is controlled by oceanic processes, especially those associated with proxies for the reduction of stratification in the Southern Ocean, but also affected by the Northern Hemisphere climate. Reductions in overturning circulation in the Northern Hemisphere appear to be associated with increases in atmospheric CO_2. On the basis of these data, if global warming causes a decrease in the overturning circulation (*32*), we might expect a positive feedback from additional CO_2 emissions to the atmosphere. However, the application of those observations to the future carbon cycle should be done cautiously because of differences between glacial and interglacial climate boundary conditions (*17*). It is likely that higher-resolution records of CO_2 will reveal more details about precise timing between Antarctic and Greenlandic temperature and atmospheric CO_2.

References and Notes

1. W. Dansgaard *et al.*, *Nature* **364**, 218 (1993).
2. P. M. Grootes, M. Stuiver, J. W. C. White, S. J. Johnsen, J. Jouzel, *Nature* **366**, 552 (1993).
3. G. Bond *et al.*, *Nature* **365**, 143 (1993).
4. T. Blunier, E. J. Brook, *Science* **291**, 109 (2001).
5. EPICA Community Members, *Nature* **444**, 195 (2006).
6. A. Ganopolski, S. Rahmstorf, *Nature* **409**, 153 (2001).
7. T. F. Stocker, S. J. Johnsen, *Paleoceanography* **18**, 10.1029/2003PA000920 (2003).
8. B. Stauffer *et al.*, *Nature* **392**, 59 (1998).
9. A. Indermühle, E. Monnin, B. Stauffer, T. F. Stocker, M. Wahlen, *Geophys. Res. Lett.* **27**, 735 (2000).
10. Materials and methods are available as supporting material on *Science* Online.
11. J. Ahn, E. J. Brook, *Geophys. Res. Lett.* **34**, L10703 10.1029/2007GL029551 (2007).
12. J. Severinghaus, A. Grachev, M. Spencer, R. Alley, E. J. Brook, *Geophys. Res. Abstr.* **5** (suppl.), 04455 (2003); available at www.cosis.net/abstracts/EAE03/04455/EAE03-J-04455.pdf.
13. C. Huber *et al.*, *Earth Planet. Sci. Lett.* **243**, 504 (2006).
14. A. Grachev, E. J. Brook, *Geophys. Res. Lett.* **34**, L20703, 10.1029/2007GL029799 (2007).
15. O. Marchal, T. F. Stocker, F. Joos, *Paleoceanography* **13**, 225 (1998).
16. A. Schmittner, E. J. Brook, J. Ahn, in *Ocean Circulation: Mechanisms and Impacts*, A. Schmittner, J. Chiang, S. Hemming, Eds. (AGU Geophysical Monograph Series, American Geophysical Union, Washington, DC, 2007), vol. 173, pp. 315–334.
17. P. Köhler, F. Joos, S. Gerber, R. Knutti, *Clim. Dyn.* **25**, 689 (2005).
18. L. Menviel, A. Timmermann, A. Mouchet, O. Timm, *Paleoceanography* **23**, 10.1029/2007PA001445 (2008).
19. N. J. Shackleton, M. A. Hall, E. Vincent, *Paleoceanography* **15**, 565 (2000).
20. R. Robinson, A. Mix, P. Martinez, *Quat. Sci. Rev.* **26**, 201 (2007).
21. A. J. Watson, A. C. N. Garabato, *Tellus* **58B**, 73 (2006).
22. J. R. Toggweiler, J. L. Russell, S. R. Carson, *Paleoceanography* **21**, 10.1029/2005PA001154 (2006).
23. B. B. Stephens, R. F. Keeling, *Nature* **404**, 171 (2000).
24. R. Röthlisberger *et al.*, *Geophys. Res. Lett.* **31**, 10.1029/2004GL020338 (2004).
25. M. Sarnthein *et al.*, in *The Northern North Atlantic: A Changing Environment*, P. Schäfer, M. Schlüter, W. Ritzrau, J. Thiede, Eds. (Springer, New York, 2001), pp. 365–410.
26. H. Rashid, R. Hesse, D. J. W. Piper, *Paleoceanography* **18**, 10.1029/2003PA000913 (2003).
27. E. Monnin *et al.*, *Science* **291**, 112 (2001).
28. J. R. Petit *et al.*, *Nature* **399**, 429 (1999).
29. K. Kawamura *et al.*, *Nature* **448**, 912 (2007).
30. G. Winckler, R. F. Anderson, M. Q. Fleisher, D. McGee, N. Mahowald, *Science* **320**, 93 (2008).
31. F. Lambert *et al.*, *Nature* **452**, 616 (2008).
32. IPCC, *Climate Change: The Physical Science Basis. Contribution of Working Group I to the Fourth Assessment Report of the Intergovernmental Panel on Climate Change*, S. Solomon *et al.*, Eds. (Cambridge Univ. Press, New York, 2007).
33. K. B. Cutler *et al.*, *Earth Planet. Sci. Lett.* **206**, 253 (2003).
34. Y. Wang *et al.*, *Nature* **451**, 1090 (2008).

35. We thank K. Howell, Q. Ouada, J. Lee, and L. Mitchell for assistance in gas chromatographic analysis; the staff of the National Ice Core Lab for ice sampling and curation; and S. Terhune for invaluable technical assistance. We also thank P. Clark, A. Schmittner, A. Mix, N. Pisias, and J. Stoner (Oregon State University) for helpful discussions. Financial support was provided by the Gary Comer Science and Education Foundation, and NSF grants OPP 0337891 and ATM 0602395.

Supporting Online Material

www.sciencemag.org/cgi/content/full/1160832/DC1
Materials and Methods
Figs. S1 and S2
Table S1
References

22 May 2008; accepted 2 September 2008
Published online 11 September 2008;
10.1126/science.1160832
Include this information when citing this paper.